Preprints (www.preprints.org) | NOT PEER-REVIEWED | Posted: 28 February 2019 doi:10.20944/preprints201902.0262.v1

Article

Formation of Potassium 2-Hydroxy-6-naphthoate by Kolbe-Schmitt Carboxylation: A Joint Experimental and Theoretical Study

So-Jin Ahn [1], Du-Hyeon Kim [1], Eung-Gun Kim [2] and Yong-Kul Lee [1,*]

[1] Laboratory of Advanced Catalysis for Energy and Environment, Department of Chemical Engineering, Dankook University, 126 Jukjeondong, Yongin 448-701, Republic of Korea; ssorobong@naver.com (S.-J. Ahn); kart6120@naver.com(D.-H. Kim);

[2] Department of Polymer Science and Engineering, Dankook University, 126 Jukjeondong, Yongin 448-701, Republic of Korea; eg.kim@dankook.ac.kr(E.-G. Kim)

* Correspondence: yolee@dankook.ac.kr; Tel.: +82-31-8005-3466

Abstract: The reaction mechanism of the carboxylation of K-2-naphthoxide was investigated by density functional theory calculations and spectroscopic studies. The reaction intermediates and products were confirmed by CO_2 adsorbed-FTIR and ^{1}H-NMR measurements. Four steps of the reaction pathway were identified: CO_2 activation, electrophilic substitution, CO_2-K complex rearrangement, and H-shift, producing 2-hydroxy-1-naphthoic acid (2,1-HNA), 2-hydroxy-3-naphthoic acid (2,3-HNA), and 2-hydroxy-6-naphthoic acid (2,6-HNA). The occurrence of CO_2-K complex rearrangement was also confirmed. These energy profiles of reaction pathways for the reaction intermediates were well consistent the experimental results on the carboxylation of K-2-naphthoxide.

Keywords: 2-Hydroxy-6-naphthoic acid; CO_2 fixation; Carboxylation; DFT

1. Introduction

Carbon dioxide emissions have been an environmental concern for the past decades due to its greenhouse effect. Considering its abundance in various combustion processes, finding a practical method for chemical fixation of CO_2 would not only be environmentally helpful, but would also provide a cheaper source of carbon. The Kolbe-Schmitt reaction offers a direct means of CO_2 fixation on hydroxy-aromatic compounds, producing aromatic hydroxycarboxylic acids, such as salicylic acid, p-hydroxy-benzoic acid, 2-hydroxy-3-naphthoic acid (2,3-HNA), and 2-hydroxy-6-naphthoic acid (2,6-HNA). The carboxylation reaction of alkali metal phenoxides has been a subject of numerous experimental and theoretical investigations [1–6]. The reaction mechanism has been proposed by means of density functional theory (DFT) methods [2–6], and the structure of an intermediate alkali metal phenoxide- CO_2 complex has been elucidated [4]. It has been shown that the yield of the para-substituted product increases with increasing ionic radius of the alkali metal used [3,5]. A quantitative explanation for this occurrence and the equilibrium behavior of the Kolbe-Schmitt reaction has been provided [2,3]. The mechanism was also investigated by using a dimer model [6]. Alkali metal naphthoxides are another important reactant in the Kolbe-Schmitt reaction, as the resulting product of 2,6-HNA is used as an intermediate for polyesters and polymeric liquid crystals. Hence, the carboxylation reaction of alkali metal naphthoxides has drawn much interest in experimental and theoretical investigations [7–13]. Scheme 1 depicts the structure of K-2-naphthoxide and HNA isomers. Marcovic et al. theoretically examined the reaction mechanism for the carboxylation of sodium naphthoxide using DFT calculations and revealed that the carboxylation is initiated by the complexation between Na-naphthoxide and CO_2, followed by the substitution of the

© 2019 by the author(s). Distributed under a Creative Commons CC BY license.

Preprints (www.preprints.org) | NOT PEER-REVIEWED | Posted: 28 February 2019 doi:10.20944/preprints201902.0262.v1

electrophilic CO_2 at the 1- and 3-positions of the naphthalene ring [12]. They also found that the direct substitution on the 6-position is difficult due to a small ionic radius of sodium, and instead the substitution on the 8-position is possible, which is followed by the transfer of CO_2 to the 6-position to give sodium 2-hydroxy-6-naphthoate [13]. Yamaguchi et al. examined the effects of various alkali metals on the product distribution, showing that K-2-naphthoxide gives a better selectivity of 2,6-HNA (63.6%) than Na-2-naphthoxide (2.8%) [7,8]. More recently, it was demonstrated that the presence of water can decrease the production yield of 2,6-HNA in the carboxylation of K-2-naphthoxide due to the side reaction of the K-2-naphthoxide into 2-naphthol in the presence of water [8,10]. Theoretical studies of the carboxylation were also reported. DFT calculations by Marcovic et al. suggested that Na-3-naphothoxide underwent the formation of Na-3-naphothoxide-CO_2 complex at the position of C1, and further transformation to the C3 could be obtained, well in accordance with the experimental results [4,5]. On the contrary, the mechanism could not explain the greater formation of 2,6-HNA than 2,1- or 2,3-HNA, upon the introduction of K-2-naphthoxide. Although much research has been reported to increase the product selectivity and yield of 2,6-HNA via the Kolbe-Schmitt reaction, the reaction mechanism still remains unclear.

In the present study, the reaction mechanism was proposed by experimental results with varying the time of reaction progress. In order to confirm the formation of the reaction intermediate and product, particular efforts were made on the experimental demonstration using in situ FTIR and ^{1}H-NMR analysis. Moreover, the DFT calculations were used to obtain relative energy levels of reactants, intermediates, and transition state species for the carboxylation of K-2-naphthoxide to better understand the reaction mechanism.

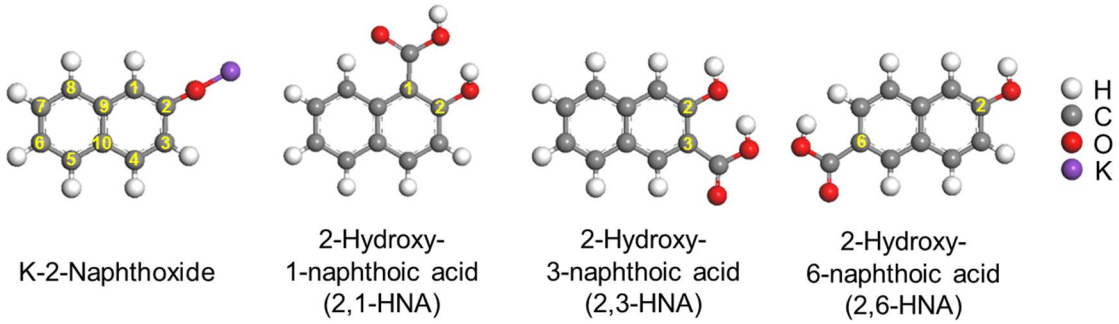

Scheme 1. The structure of K-2-naphthoxide and HNA isomers

2. Results and Discussion

2.1. Synthesis of 2,6-HNA from K-2-naphthoxide

In order to investigate the product distribution with reaction time, the carboxylation of K-2-naphthoxide was carried out at 543 K under a CO_2 pressure of 4 atm, and was monitored for 8 h at 1 or 2 h intervals. The product yields and the selectivities are given in Table. 1. With the progress of the reaction, only three HNA isomers of 2,6-, 2,3-, and 2,1-HNA, were observed. In the early stage of reaction 2,3-HNA and 2,6-HNA are generated with a product selectivity over 30% more than 2,1-HNA. It is noted that the product selectivity of 2,6-HNA is increased until the reaction time reaches 6 h, while the selectivity of 2,1-HNA and 2,3-HNA decreased. After 6 h the overall HNA yield began to decrease. These results imply that among three HNA isomers 2,6-HNA is the most favorable product in the carboxylation of K-2-naphthoxide. The product selectivity could be related with the activation mechanism of K-2-naphthoxide in the presence of carbon dioxide and the thermal stability of reaction intermediates of the reaction [2-5, 8].

Preprints (www.preprints.org) | NOT PEER-REVIEWED | Posted: 28 February 2019 doi:10.20944/preprints201902.0262.v1

Table 1 Product distribution of K-2-Naphthoxide carboxylation

Reaction Time (h)	HNA Yield (%)	2,6-HNA Yield (%)	Selectivity (%)		
			2,1-HNA	2,3-HNA	2,6-HNA
0.5	21.8	8.4	26.4	35.2	38.4
1	26.9	13.2	16.1	34.8	49.1
2	26.0	15.9	11.6	27.0	61.4
4	28.7	20.9	5.9	21.1	73.0
6	26.9	21.9	2.3	16.4	81.3
8	24.3	18.6	9.6	13.7	76.7

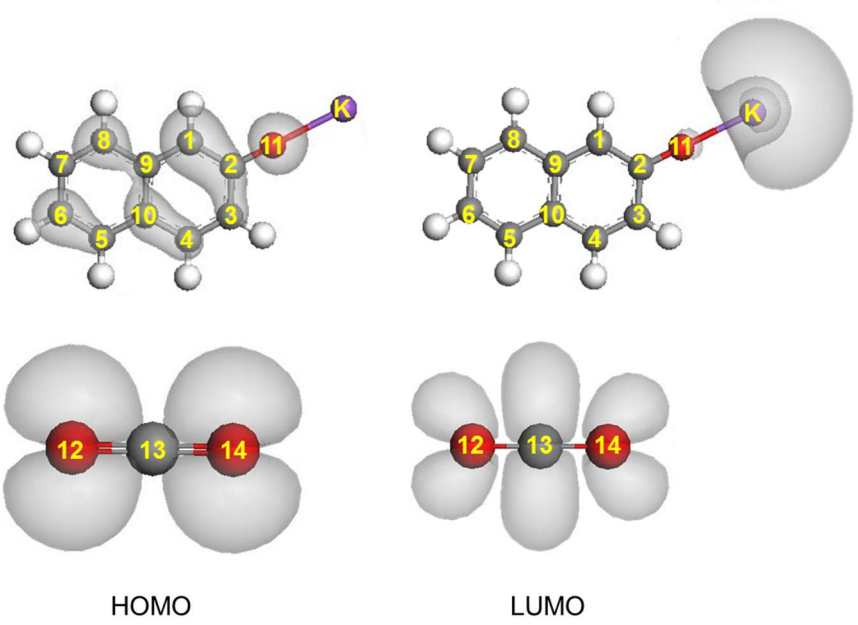

Figure 1. HOMO and LUMO of K-naphthoxide and CO_2.

2.2. Structure of the K-2-naphthoxide- CO_2 complex

Fig. 1 shows the highest occupied molecular orbitals (HOMOs) and lowest unoccupied MOs (LUMOs) of K-2-naphthoxide and CO_2. It is observed that the HOMO of K-2-naphthoxide is delocalized over the naphthalene ring and oxygen, whereas the LUMO of K-2-naphthoxide is localized mostly on the potassium atom. The HOMO of CO_2 is located on both oxygen atoms, while the LUMO of CO_2 is delocalized over all atoms with the greatest contribution from the carbon atom.

The electron charge distributions of K-2-naphthoxide and K-2-naphthoxide-CO_2 complex were also calculated and the results are summarized in Table 2. It can be seen that the oxygen and carbons of the naphthalene ring (except for the C2, C9, and C10), especially C1, C3, and C6, are negatively charged, whereas the positive charge is highly distributed between the potassium and C2. As expected, the carbon of CO_2 is positively charged, whereas the negative charge is distributed between the oxygen. These charge distribution analysis clearly indicates that the oxygen and carbon of CO_2 would combine with the potassium and the adjacent oxygen of K-2-naphthoxide, respectively, thus forming K-2-naphthoxide-CO_2 complex.

In order to confirm the CO_2 activation step, in situ FTIR analysis of CO_2 absorption on the dried K-2-naphthoxide was conducted as presented in Fig. 2 (a). After CO_2 injection at 323 K, a strong peak appeared at 2365 cm^{-1} with a broad shoulder at around 2340 cm^{-1}, while the peak intensities decreased with a N_2 purge. This result indicates that the CO_2 is weakly bonded to K-2-naphthoxide. The broad shoulder observed in 2400-2300 cm^{-1} is assigned to the asymmetric stretching mode of gas phase CO_2. The splitting of the mode is due to coupling with rotational energy modes. The calculated IR

Preprints (www.preprints.org) | NOT PEER-REVIEWED | Posted: 28 February 2019 doi:10.20944/preprints201902.0262.v1

spectra of K-2-naphthoxide-CO_2 complex (Fig. 2 (b)) also retain the peak of CO_2 vibration near the O-K bond at 2280 cm^{-1}, indicating the formation of complex between K-2-naphthoxide and CO_2. Similar discrepancies between experimental and normal mode analysis were also found for the Na-phenoxide-CO_2 complex, which came from computational error. The vibrational frequency calculation is commonly based on the potential energy surfaces harmonic oscillator, while the reality is anharmonic. This results in the vibrational frequency overestimating even by 20 % [4].

Table 2 Population analysis (electron charges) on the selected atoms in reactants and intermediates.

	2-naphthol	K-2-naphthoxide	K-naph-CO_2 complex
C(1)	-0.115	-0.155	-0.143
C(2)	0.342	0.293	0.302
C(3)	-0.063	-0.118	-0.110
C(4)	-0.022	-0.072	-0.072
C(5)	-0.034	-0.073	-0.074
C(6)	-0.021	-0.095	-0.091
C(7)	-0.012	-0.075	-0.074
C(8)	-0.041	-0.086	-0.085
C(9)	0.101	0.042	0.043
C(10)	0.081	0.014	0.017
O(11)	-0.463	-0.719	-0.751
K	-	0.809	0.831
O(12)	-	-	-0.262
C(13)	-	-	0.611
O(14)	-	-	-0.412

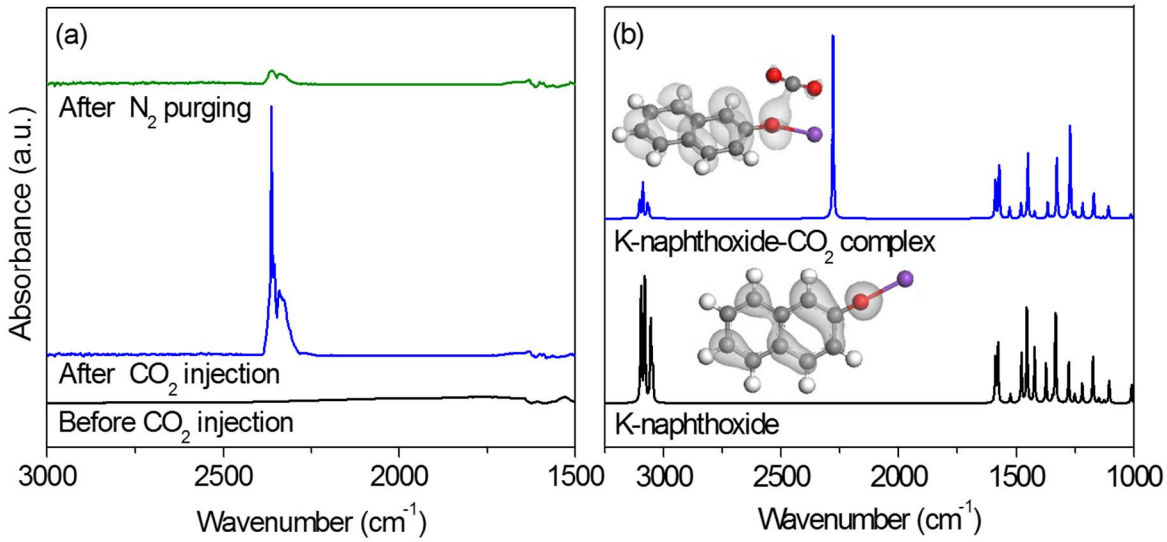

Figure 2. In situ FTIR spectra of K-2-naphthoxide-CO_2 complex (a) and computational vibration spectra (b)

2. 3. Reaction Mechanisms of K-2-naphthoxide Carboxylation

Fig. 3 shows possible scenarios of the reaction mechanism along with the energetic diagram of K-2-naphthoxide carboxylation, where the carboxylation of K-2-naphthoxide could undergo three reaction pathways, resulting in 2,1-HNA, 2,3-HNA, and 2,6-HNA. Reaction paths 1 and 2 are the

Preprints (www.preprints.org) | NOT PEER-REVIEWED | Posted: 28 February 2019 doi:10.20944/preprints201902.0262.v1

representative Kolbe-Schmitt reaction pathways in which CO_2 is directly substituted at the C1 and C3 positions, respectively, whereas reaction path 3 includes a dimer model where CO_2 activated by a K-2-naphthoxide can be substituted at C6 position of the other K-2-naphthoxide, i.e. intermolecular substitution. Each reaction pathway consists of three intermediates for CO_2 substitution (step I), K-rearrangement (step II), and H-shift (step III), undergoing three respective transition states of TS-1, 2, and 3, and two intermediate species i.e., IM-1 and 2.

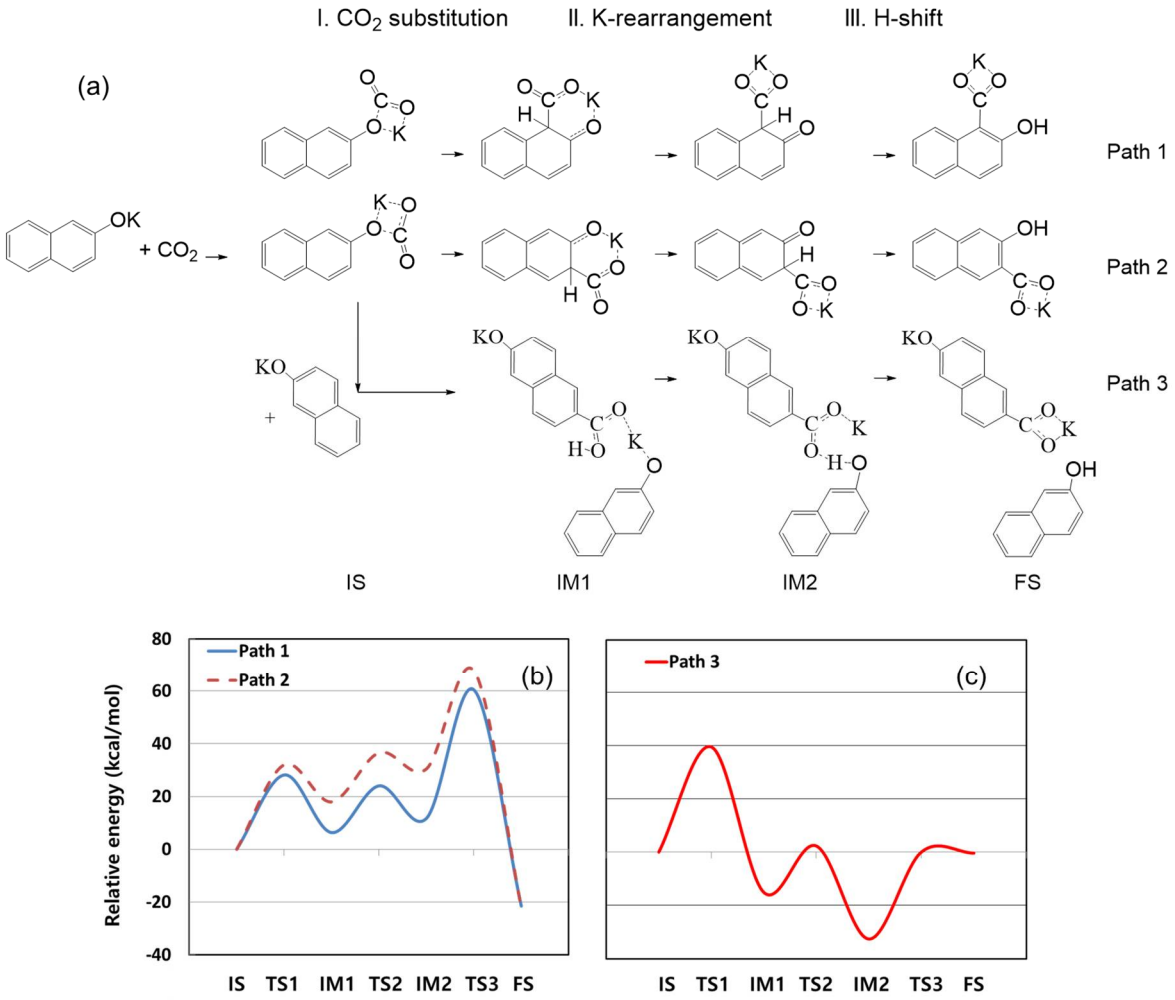

Figure 3. Proposed reaction pathways (a) and **e**nergy profiles of K-2-naphthoxide carboxylation (b,c)

The calculation results are given in Fig. 3 and Table 3. The imaginary frequencies and thermodynamic properties of the species in the reaction paths are summarized in Table S1-3 of supplementary materials. The relative energy profiles displayed in Fig. 3(b) indicate that the CO_2 substitution on to C1 and C3, i.e. step I, is found to proceed with activation barriers (TS1) of 28.171 and 32.045 kcal/mol, respectively. However, the direct CO_2 substitution on to C6 position was not possible. Similar results were reported for the CO_2 substitution on Na-2-naphthoxide [2–5,12], where the direct CO_2 substitution on Na-2-naphthoxide could not proceed at the C6 position. These results may be due to a longer distance between C6 and C2 positions [1,3]. The ionic radius of cations are also known to affect carboxylation product selectivities, as found in the synthesis of salicylic acid, where a smaller cation like Na leads to the CO_2 substitution only in the nearest ortho-position, while larger cations like K and Cs favor the para-substitution [4,5]. For the carboxylation on to C6 position, given a longer distance between C2 and C6 of K-naphthoxide, i.e. 5.12 Å, the intermolecular carboxylation can be considered rather than the intramolecular carboxylation as illustrated in

Preprints (www.preprints.org) | NOT PEER-REVIEWED | Posted: 28 February 2019 doi:10.20944/preprints201902.0262.v1

reaction path 3 of Fig. 3(a). The calculation results show that the CO_2 substitution on to C6 position of K-naphthoxide can be achieved by an adjacent CO_2-K-naphthoxide complex with a slightly higher activation energy of 39.464 kcal/mol. The energy profiles may result from different electron density and distance between the activated carbon atom of CO_2 and each carbon atom of K-2-naphthoxide. These results thus imply that in the early stage of reaction CO_2 substitution in the nearest C3 position can preferentially be facilitated, followed by C1 and C6 position. For the following K-rearrangement step (step II), the activation energy barriers (TS2) of the three products (Fig. 3 (b,c)) are found to follow the order, 2,3-HNA (18.680 kcal/mol) > 2,1-HNA (17.692 kcal/mol) > 2,6-HNA (17.431 kcal/mol). It can be noted that the intermolecular CO_2 rearrangement provides the lowest energy barrier among the three paths. For the H-shift reaction (step III), the activation energy barriers (TS3) of the three products (Fig. 3 (b,c)) followed the order, 2,1-HNA (48.715 kcal/mol) > 2,3-HNA (37.360 kcal/mol) > 2,6-HNA (32.627 kcal/mol). Again, the intermolecular pathway provides the lowest energy barrier among the three paths. These results thus suggest that the formation of more 2,6-HNA can occur with the reaction progress. The reaction test results given in Table 1 are in line with the theoretical calculations, supporting the gradual increasing trend of 2,6-HNA formation with the reaction progress.

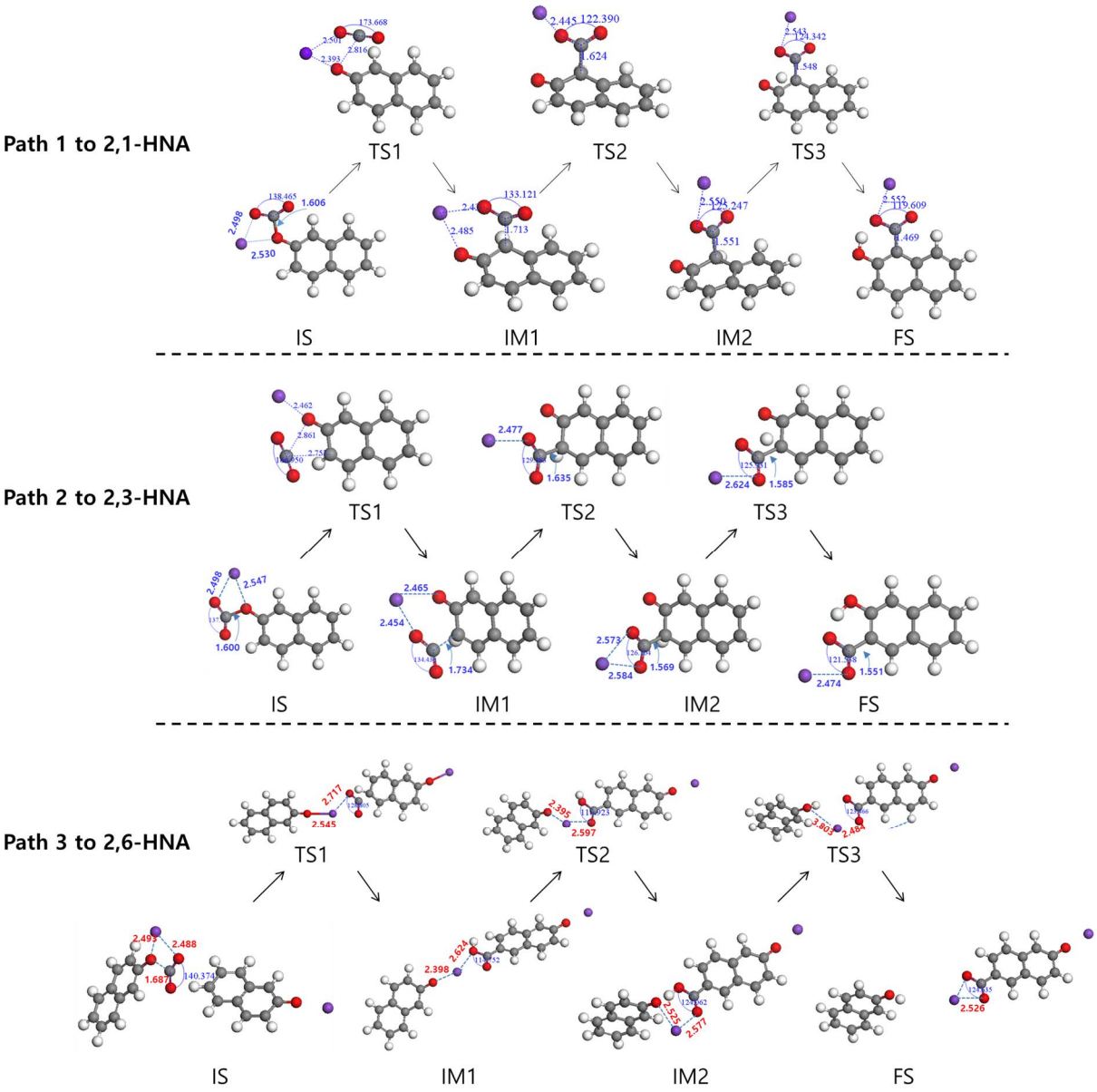

Figure 4. Optimized geometries of reactants, intermediates, and transition states for carboxylation of K-2-naphthoxide.

Preprints (www.preprints.org) | NOT PEER-REVIEWED | Posted: 28 February 2019 doi:10.20944/preprints201902.0262.v1

Fig. 4 shows the proposed reaction pathways with the optimized geometries of the intermediates 1 and 2 and transition states 1, 2, and 3 of the reaction paths. After the vibration frequencies were analyzed for the optimized geometry, the standard molar enthalpies, and standard molar Gibbs free energies were obtained and listed in Table S1-S3, and the activation energy and the thermodynamic state functions for each reaction were calculated as presented in Table 3. Although the paths 1 and 2 show a lower activation energy for the CO_2 substitution step than the path 3, the path 3 presents a much lower activation energies for the following K-rearrangement and H-shift steps. The calculation results also indicate that the carboxylation is exothermic reaction with a standard molar reaction heat of 1.89-20.80 kcal/mol, and shows negative Gibbs free energies in all paths. In contrast, the paths 1 and 2 undergo entropy loss reactions more than the path 3. The reaction path 2 seems energetically more favorable with respect to ΔH_r^o and ΔG_r^o, however the path 3 provides lower activation barriers in steps II and III. These results indicate that the intermolecular carboxylation pathway is a favorable route in view of kinetics.

Table 3 The activation energies and thermodynamic state functions of the three reaction paths.

	Path 1	Path 2	Path 3
E_a (TS1/TS2/TS3, kcal/mol)	28.171 / 17.692 / 48.715	32.045 / 18.680 / 37.360	39.464 / 17.431 / 32.627
ΔH_r (298/543K, kcal/mol)	-20.80/-21.32	-20.26/-20.39	-1.89/-2.09
ΔG_r (298/543K, kcal/mol)	-18.66/-16.66	-19.79/-22.41	-1.56/-1.22
ΔS_r (298/543K, cal/molK)	-7.19/-8.59	-1.58/3.71	-1.11/-1.59

$\Delta H_r = \Sigma[H(T)+E_{0K}]_{product}-\Sigma[H(T)+E_{0K}]_{reactant}$; $\Delta G_r =\Sigma[G(T)+E_{0K}]_{product}-\Sigma[G(T)+E_{0K}]_{reactant}$; $\Delta S_r =[\Delta H_r -\Delta G_r]/T$

In order to identify the reaction products, ^{1}H-NMR analysis was employed. The reaction products of K-2-naphthoxide carboxylation were analyzed together with 2-naphthol, 2,1-HNA, 2,3-HNA, and 2,6-HNA as references, as displayed in Fig. 5. The NMR bands for O-H and COOH were assigned at 9.5-10 ppm and 11-14 ppm, respectively. The NMR spectra of the reaction product collected after reaction at 6 h exhibited O-H band without the formation of COOH band. These results suggest that the products of the carboxylation retain COOK group instead of COOH after the reaction.

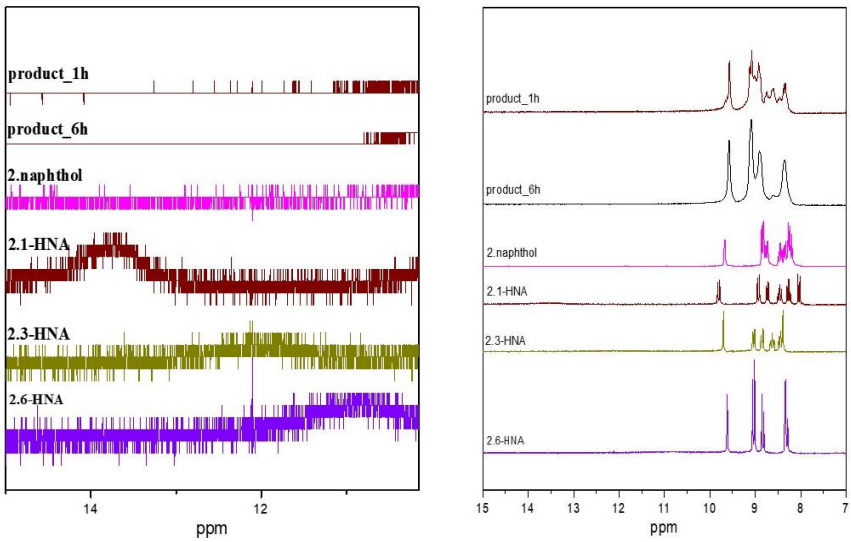

Figure 5. ^{1}H-NMR of reactant, and product for K-2-naphthoxide carboxylation.

Based upon the findings about the nature of the K-2-naphthoxide and the energy profiles of reaction pathways the reaction mechanism for the carboxylation of K-2-naphthoxide can be proposed

Preprints (www.preprints.org) | NOT PEER-REVIEWED | Posted: 28 February 2019 doi:10.20944/preprints201902.0262.v1

as presented in Fig. 6. The reaction mechanism captures the essential features of the carboxylation: the involvement of CO_2 activation, the occurrence of electrophilic substitution, CO_2-K complex rearrangement, and H-shift. Moreover, the formation of 2,6-HNA was confirmed by intermolecular substitution pathways.

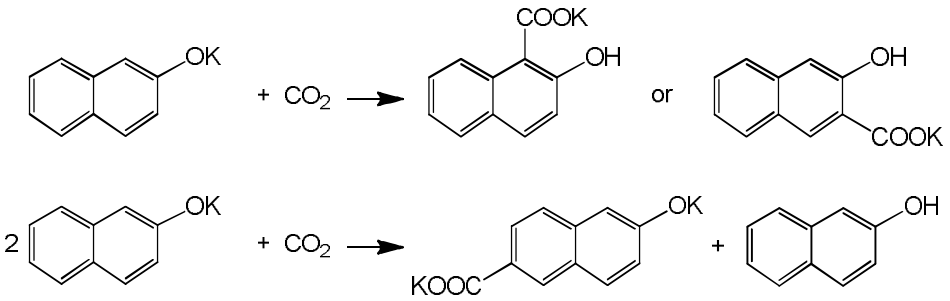

Figure 6. Proposed reaction mechanism of K-2-naphthoxide carboxylation.

3. Experimental and Computational Methods

3.1. Materials and Reaction Tests

The general procedure to synthesize the HNA's is as follows: in preparing K-2-naphthoxide, 6.8 mmol 2-naphthol (Sigma Aldrich, 98%), 6.8 mmol potassium hydroxide (KOH), and 5 ml water were mixed and stirred at room temperature for 1 h. The mixture was combined with hexadecane (Tokyo Chemical Industry, 98%) of 20 ml in a 100 ml autoclave. The autoclave was heated to 513 K under a slow purge of N_2 for 40 min to remove water and heated to 543 K, charged with CO_2 by 4 atm, and then maintained for 6 h [10]. The product was analyzed by high performance liquid chromatography (HPLC pump: Lab alliance series 1500; UV/VIS detector (254 nm): Hitachi L-7400; column: Inertsil ODS-2, 4.6 Φ x 250 mm; solvent: A mixture of acetonitrile and water (50:50, v/v), which was slightly acidified by the addition of 1% acetic acid).

3.2. In situ FTIR and ^{1}H-NMR Measurements

Infrared spectra of pressed wafers (~15 mg) of samples were collected in situ in an infrared (IR) reactor cell placed in a FTIR spectrometer (Frontier FTIR, PekinElmer) at a resolution of 2 cm^{-1} and using 64 scans $spectrum^{-1}$. A mass of 20-30 mg of the 10 wt% K-2-naphthoxide diluted in KBr was pressed by 30 MPa, and the sample wafer was put on the in situ FTIR cell. The cell was heated to 373 K along with evacuation and maintained for 30 min to remove moisture, and was cooled down to 323 K to collect background spectrum. For measurement, 10 wt% CO_2/N_2 was introduced into the cell till the saturation being attained. Then, the flow was switched to N_2 to obtain the IR spectra of the absorbed species.

^{1}H-NMR spectra for measured reactant, primary and final product, and references of 2,1-HNA, 2,3-HNA, and 2,6-HNA.were obtained by Variann 200MHz EM-360. For measurement, the samples were dissolved in D_2O.

3.3. Computational Methods

Calculations were performed using Dmol3 package [14,15] based on the density functional theory. For the DFT calculations the BLYP of the generalized gradient approximation (GGA) was used for the electron exchange and correlation [16]. The convergence criterion for the charge density of self-consistent iterations was set to 10^{-5}. Geometrical optimizations were carried out for reactant,

Preprints (www.preprints.org) | NOT PEER-REVIEWED | Posted: 28 February 2019 doi:10.20944/preprints201902.0262.v1

intermediate, and product species, using the DNP/3.5 basis set. After then, the optimized structures of each species were selected as reactants or products for synchronous transit methods, which we used to locate the transition state. The transition state was then obtained for each reaction step, and harmonic vibration frequencies were also calculated for the intermediate species. The Mulliken charges on each atom were also calculated by the Mulliken population analysis.

4. Conclusions

The carboxylation of K-2-naphthoxide has been well understood by the DFT calculations and spectroscopic studies. CO_2 was easily activated on K-2-naphthoxide with a very low activation barrier. The initial formation of K-2-naphthoxide-CO_2 complex was confirmed by DFT calculation and also by in-situ FTIR analysis with the CO_2 adsorption. The carbon of CO_2 in the K-2-naphthoxide-CO_2 complex underwent an electrophilic attack on the naphthalene ring, especially on the high electron density carbon such as C1, C3, and C6, followed by CO_2-K complex rearrangement, and H-shift, resulting in the formation of 2,1-HNA, 2,3-HNA, and 2,6-HNA. The high product selectivity of 2,6-HNA was well estimated by intermolecular substitution pathway, which provides lower activation energies.

Acknowledgements

This research was funded by Dankook University in 2016.

References

1. Kosugi, Y.; Imaoka, Y.; Gotoh, F.; Rahim, M.A.; Matsui, Y.; Sakanishi, K. Carboxylations of alkali metal phenoxides with carbon dioxide. *Org. Biomol. Chem.* **2003**, *1*, 817–821.
2. Marković, Z.; Engelbrecht, J.P.; Marković, S. Theoretical study of the Kolbe-Schmitt reaction mechanism. *Zeitschrift fur Naturforsch. - Sect. A J. Phys. Sci.* **2002**, *57*, 812–818.
3. Markovic, Z.; Markovic, S.; Begovic, N. Influence of alkali metal cations upon the kolbe-schmitt reaction mechanism. *J. Chem. Inf. Model.* **2006**, *46*, 1957–1964.
4. Markovic, Z.; Markovic, S.; Manojlovic, N.; Predojevic-Simovic, J. Mechanism of the Kolbe - Schmitt Reaction . Structure of the Intermediate Potassium Phenoxide - CO 2 Complex. *J. Chem. Inf. Model.* **2007**, 1520–1525.
5. Markovic, S.; Markovic, Z.; Begovic, N.; Manojlovic, N. Mechanism of the Kolbe-Schmitt reaction with lithium and sodium phenoxides. *Russ. J. Phys. Chem. A* **2007**, *81*, 1392–1397.
6. Yamabe, S.; Yamazaki, S. An unsymmetrical behavior of reactant units in the Kolbe-Schmitt reaction. *Theor. Chem. Acc.* **2011**, *130*, 891–900.
7. Iijima, T.; Iwase, T.; Yamaguchi, T. Carboxylation of 2-Naphthol with Carbon Dioxide in Anisole. **2006**, *209*, 206–209.
8. Iijima, T.; Takagi, D.; Yamaguchi, T. Carboxylation of 2-Naphthol in Kerosene. **2008**, *51*, 65–69.
9. Ueno, R.; Sakota, K. JP 195599/81 1981.
10. Ueno, R.; Masada, Y. JP 86-176254 1986.
11. Hautzel, Z.; Main, F.A.; Rittner, S.; Walldorf, M. US 5312974 1994.
12. Marković, Z.; Marković, S.; Crossed D Signurović, I. Kolbe-Schmitt reaction of sodium 2-naphthoxide. *Monatshefte fur Chemie* **2008**, *139*, 329–335.
13. Marković, S.; Durović, I.; Marković, Z. Formation of sodium 6-hydroxy-2-naphthoate in the Kolbe-Schmitt reaction. *Monatshefte fur Chemie* **2008**, *139*, 1169–1174.
14. Delley, B. Analytic energy derivatives in the numerical local-density-functional approach. *J. Chem. Phys.* **1991**, *94*, 7245–7250.

Preprints (www.preprints.org) | NOT PEER-REVIEWED | Posted: 28 February 2019 doi:10.20944/preprints201902.0262.v1

15. Delley, B. An all-electron numerical method for solving the local density functional for polyatomic molecules. *J. Chem. Phys.* **1990**, *92*, 508–517.
16. Laird, B.B.; Ross, R.B.; Ziegler, T. Density-Functional Methods in Chemistry: An Overview. **1996**, 1–17.